Mechanistic insights from plant heteromannan synthesis in yeast

Cătălin Voiniciuc[a,1], Murali Dama[a], Niklas Gawenda[a], Fabian Stritt[a], and Markus Pauly[a,2]

[a]Institute for Plant Cell Biology and Biotechnology, Heinrich Heine University, 40225 Düsseldorf, Germany

Edited by Kenneth Keegstra, Michigan State University, East Lansing, MI, and approved November 28, 2018 (received for review August 14, 2018)

Heteromannan (HM) is one of the most ancient cell wall polymers in the plant kingdom, consisting of β-(1–4)-linked backbones of glucose (Glc) and mannose (Man) units. Despite the widespread distribution of HM polysaccharides, their biosynthesis remains mechanistically unclear. HM is elongated by glycosyltransferases (GTs) from the cellulose synthase-like A (CSLA) family. MANNAN-SYNTHESIS RELATED (MSR) putative GTs have also been implicated in (gluco)mannan synthesis, but their roles have been difficult to decipher *in planta* and in vitro. To further characterize the products of the HM synthases and accessory proteins, we chose a synthetic biology approach to synthesize plant HM in yeast. The expression of a CSLA protein in *Pichia pastoris* led to the abundant production of plant HM: up to 30% of glycans in the yeast cell wall. Based on sequential chemical and enzymatic extractions, followed by detailed structural analyses, the newly produced HM polymers were unbranched and could be larger than 270 kDa. Using CSLAs from different species, we programmed yeast cells to produce an HM backbone composed exclusively of Man or also incorporating Glc. We demonstrate that specific MSR cofactors were indispensable for mannan synthase activity of a coffee CSLA or modulated a functional CSLA enzyme to produce glucomannan instead of mannan. Therefore, this powerful platform yields functional insight into the molecular machinery required for HM biosynthesis in plants.

plant cell wall | polysaccharide | glycosyltransferase | mannan | yeast

Plants thrive in a wide range of aqueous and terrestrial environments, as their cells are shaped and reinforced by a carbohydrate-rich extracellular matrix. Plant cell wall polysaccharides make up the bulk of plant biomass, and thus represent the most abundant source of renewable material on the planet (1). One class of wall polysaccharides, the hemicelluloses, are a heterogenous group of polysaccharides consisting of β-(1–4)-linked backbones of glucose (Glc), mannose (Man), or xylose units (2). In addition to strengthening the wall, hemicelluloses facilitate cell expansion, store carbohydrates, and supply signal molecules in certain tissues (2). Heteromannan (HM) is regarded as the most ancient type of hemicellulose, and is found throughout the plant kingdom, including in red algae (3), early land plants (mosses, lycophytes), gymnosperms, and angiosperms (4). Along with these important biological functions, HM is important for human nutrition, and may play a role in the treatment of lifestyle diseases such as type 2 diabetes (5). In addition, HM polysaccharides are widespread ingredients used to stabilize foods and cosmetics, coat pharmaceutical drugs for the controlled release of active agents, and even waterproof dynamite sticks for the mining industry (6). The global demand for HM has increased substantially in recent years because of its utility as a fluid thickener in hydraulic fracturing for oil and gas (7). Despite the widespread distribution and important applications of HM, the roles of genetic factors that determine the polysaccharide's fine structure remain to be characterized.

Changes in HM monosaccharide composition, length, or substitution modulate the polymer's physical properties and determine, for instance, whether a polysaccharide forms a crystalline aggregate or is water-soluble. Two distinct HM backbones are found in plants (2): linear mannan consists almost exclusively (>90%) of Man subunits, whereas glucomannan also includes Glc residues. Mannan accumulates primarily in palm seeds, whereas glucomannan is more widespread and is, for example, highly enriched in konjac corms (8). The solubility of HM polysaccharides is enhanced by the substitution of Man units in (gluco)mannan with galactose side chains. For example, coffee seeds accumulate a galactosyl-substituted mannan (9), whereas galactoglucomannan is the most abundant hemicellulose in softwood (10).

Similar to other plant hemicelluloses, HM is synthesized by Golgi-localized glycosyltransferases (GTs), and the resulting polysaccharides are secreted to the plant cell wall via exocytosis. GTs from the Cellulose Synthase-Like A (CSLA) family have been demonstrated to use GDP-Man, and sometimes GDP-Glc, to elongate the HM backbone in vitro (11–14), but the polymers made by different CSLA isoforms have not been characterized in detail. In addition, MANNAN-SYNTHESIS RELATED (MSR) putative GTs are associated with (gluco)mannan synthesis (15, 16), but their roles have been difficult to decipher *in planta* and in vitro. *Arabidopsis thaliana* (*At*) MSRs have been hypothesized to synthesize a primer to initiate HM synthesis, glycosylate CSLA enzymes to enhance their activity, or promote CSLA stability or activity via glycosylation-independent interactions (15). Because these hypotheses have not been tested, the machinery that synthesizes different HM types remains unclear.

To further characterize the products of CSLA enzymes and the roles of accessory proteins such as MSR, we genetically engineered yeast to synthesize and secrete plant HM to their

Significance

Heteromannans are ancient plant cell wall polysaccharides, ubiquitous throughout the plant kingdom. In plants, these hemicellulosic polymers strengthen the cell wall and facilitate energy storage, and are involved in cell expansion and developmental signaling. Heteromannans are used extensively by humans, as healthy dietary fibers and as thickening agents in food, cosmetic, pharmaceutical, and mining industries. The fine structure of heteromannan is important for the polysaccharide's biophysical properties, and thus its function and application. However, the biosynthesis of different heteromannan structures remains mechanistically unclear. We demonstrate that plant mannan and glucomannan can be synthesized heterologously in the yeast *Pichia pastoris*, and the polysaccharide's structure can be modulated by specific plant cofactors, allowing for the synthesis of tailored mannan structures.

Author contributions: C.V. and M.P. designed research; C.V., M.D., N.G., and F.S. performed research; C.V., M.D., N.G., F.S., and M.P. analyzed data; and C.V. and M.P. wrote the paper.

The authors declare no conflict of interest.

This article is a PNAS Direct Submission.

[1]Present address: Independent Junior Research Group–Designer Glycans, Leibniz Institute of Plant Biochemistry, 06120 Halle (Saale), Germany.

[2]To whom correspondence should be addressed. Email: m.pauly@hhu.de.

This article contains supporting information online at www.pnas.org/lookup/suppl/doi:10.1073/pnas.1814003116/-/DCSupplemental.

walls. *Pichia pastoris* (hereafter *Pichia*) was selected as a promising host because it only contains trace amounts of 4-linked Man in its wall (17), and active CSLA proteins have been expressed in this host for in vitro assays (8, 18). Related Cellulose Synthase-Like C enzymes that elongate the backbone of xyloglucan, another type of hemicellulose, were also functional in *Pichia* (17). We now show that CSLA expression in *Pichia* led to the abundant production of plant HM. Depending on the CSLA isoform used, yeast cells synthesized linear HM polymers built primarily of Man, or also incorporating Glc. Using this platform, we demonstrate that MSR proteins are important cofactors for the elongation and the composition of plant mannan and glucomannan.

Results

Engineering *Pichia* to Produce Plant HM in Its Cell Wall. We engineered *Pichia* cells to produce plant HM to characterize the polysaccharides produced by CSLA enzymes and the roles of MSR proteins. As a proof of concept, we stably integrated the *Amorphophallus konjac* (*Ak*) *CSLA3* coding sequence in the *Pichia* genome under the control of a methanol-inducible promoter. This gene was selected because *Pichia* microsomes expressing recombinant AkCSLA3 have glucomannan synthase activity in radiometric assays (8). *Pichia* cells containing the *AkCSLA3* transgene were grown for biomass production before inducing recombinant protein expression. *Pichia* cell wall alcohol-insoluble residue (AIR) was isolated and subjected to glycosidic linkage analysis. The wall AIR of an empty vector control *Pichia* strain was rich in 2-Man and 3-Glc linkages, derived from native yeast α-mannoproteins and β-1,3-glucans, respectively, but only contained trace amounts of 4-Man (Fig. 1*A* and *SI Appendix*, Fig. S1*A*). The expression of AkCSLA3 led to the abundant production of 4-Man, characteristic of plant mannan, and also showed an increased 4-Glc content (Fig. 1*A* and *SI Appendix*, Fig. S1*A*). The abundance of 4-Man was elevated up to 30% of total carbohydrates in the AkCSLA3 cell wall AIR (Fig. 1*A*). To confirm the stability of HM production in yeast cells, an AkCSLA3 colony examined in Fig. 1*A* was reanalyzed alongside five additional AkCSLA3 colonies (*SI Appendix*, Fig. S1*B*), isolated from an independent transformation. Indeed, 4-Man was the dominant wall glycosidic linkage for all AkCSLA3 transformants (*SI Appendix*, Fig. S1*B*). In contrast to its effects on wall AIR, AkCSLA3 did not alter the composition of ethanol-precipitable glycans secreted in the culture media (*SI Appendix*, Fig. S1*C*).

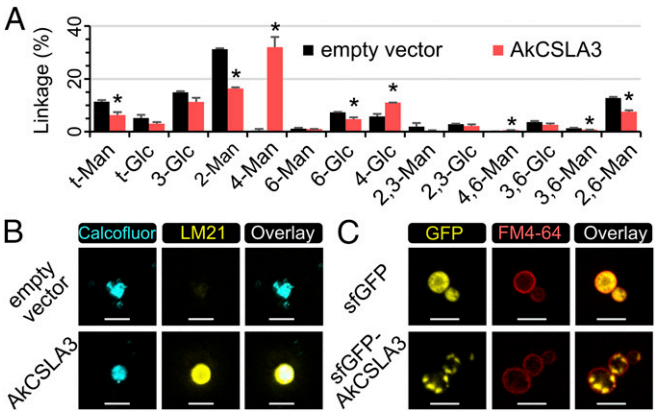

Fig. 1. Yeast cells expressing AkCSLA3 accumulate plant HM in their walls. (*A*) Glycosidic linkage analysis of *Pichia* wall AIR. Values represent molar percentage of total carbohydrates detected. Data show mean + SD of two independent transformants for each strain. Asterisks indicate significant changes (two-tailed *t* test, $P < 0.05$) between the strains. (*B*) Yeast wall polysaccharides with stained with calcofluor, a general β-glucan dye, and immunolabeled with the HM-binding LM21 antibody. (*C*) Subcellular localization of AkCSLA3 enzymes in *Pichia* cells. The plasma membrane was stained with the FM4-64 dye. The signal intensity of all channels for the fusion protein sfGFP-AkCSLA3 sample was increased postacquisition, relative to sfGFP control. (Scale bars, 5 μm.)

To investigate whether the products of AkCSLA3 were deposited in the yeast cell wall, *Pichia* spheroplasts were immunolabeled with LM21 and LM22, two HM-specific monoclonal antibodies (19) that cannot cross the plasma membrane. The AkCSLA3 cells were labeled by LM21 or, to a lesser extent, LM22 antibodies (*SI Appendix*, Fig. S2 *A–C*). Although LM21 epitopes were only detected in AkCSLA3-expressing cells, native yeast β-glucans were stained in a similar fashion by the calcofluor dye in both the AkCSLA3 and empty vector *Pichia* strains (*SI Appendix*, Fig. S2 *D–G*). Confocal microscopy confirmed that the LM21 signals detected in the AkCSLA3-expressing cells colocalized with the yeast wall counterstained with calcofluor (Fig. 1*B*). The subcellular localization of the AkCSLA3 enzyme was investigated using a superfolder green fluorescent protein (sfGFP) N-terminal tag (20). Although the free sfGFP tag was distributed throughout the cytosol (*SI Appendix*, Fig. S2*H*), the sfGFP-AkCSLA3 fusion proteins were localized in small punctae (*SI Appendix*, Fig. S2*I*), interior to the plasma membrane stained by FM4-64 (Fig. 1*C*). The sfGFP-AkCSLA3 protein was functional, but AkCSLA3 yielded more HM sugars (*SI Appendix*, Fig. S2*J*), so only untagged proteins were expressed in further experiments. Therefore, as observed in plants, *Pichia* cells expressed CSLA recombinant proteins in intracellular compartments, but deposited their HM products in the extracellular matrix.

Product Specificity of CSLA Enzymes from Different Species. The products of AkCSLA3 and the *At* CSLA2 protein were compared to investigate whether different CSLA isoforms yield distinct HM structures, When expressed in *Pichia*, the two enzymes produced equally high amounts of 4-Man in the wall AIR, but only AkCSLA3 significantly increased the content of 4-Glc relative to the empty vector control (Fig. 2*A*). This suggests that the AkCSLA3 enzyme produces glucomannan, but AtCSLA2 synthesizes a relatively pure mannan in yeast. We enriched the novel HM polysaccharides by washing the cell wall AIR with hot 1 M sodium hydroxide (*SI Appendix*, Fig. S3*A*), which removes yeast α-mannoproteins (21). The resulting alkaline-insoluble (AKI) material was then treated with Zymolyase, which digests yeast β-1,3-glucans proteins (21), to yield an enriched HM (EM) fraction (*SI Appendix*, Fig. S3*A*). These sequential extractions removed most of the native yeast polymers, and thus enriched the CSLA product (*SI Appendix*, Fig. S3*B*). The EM polysaccharides were enzymatically characterized using purified β-mannanase and cellulase recombinant enzymes, which cleave β-1,4-Man and β-1,4-Glc bonds, respectively. Relative to the empty vector and undigested samples, the AkCSLA3 protein produced HM polymers that could be digested by β-mannanase and, to a lesser extent, cellulase treatment (Fig. 2*B*). In contrast, the AtCSLA2 product was only digested by β-mannanase (Fig. 2*B*), indicating a lack of β-1,4-Glc bonds. To further investigate their structure, EM polysaccharides were subjected to proton NMR (^{1}H-NMR) spectroscopy (Fig. 3*C*), alongside standards for plant HM polymers and yeast glucans (*SI Appendix*, Table S2). No carbohydrate peaks were observed in the ^{1}H-NMR spectrum of the empty vector control (Fig. 3*C*). The ^{1}H-NMR spectrum of the EM polymers made by AkCSLA3 contained the anomeric peaks characteristic of β-1,4-glucan and β-1,4-mannan (Fig. 3*C*), as well as other aliphatic signals also found in konjac glucomannan (*SI Appendix*, Table S2). In contrast, the AtCSLA2 product lacked the β-1,4-glucan anomeric peak (Fig. 3*C*), but had signals with the identical chemical shifts as pure mannan extracted from ivory nut (*SI Appendix*, Table S2). Therefore, *Pichia* cells expressing AkCSLA3 and AtCSLA2 produced glucomannan and mannan, respectively.

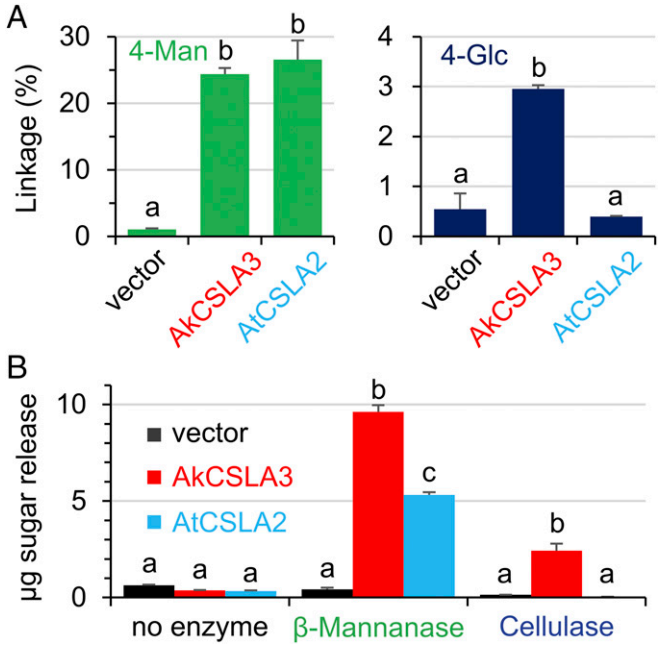

Fig. 2. Products after AkCSLA3 and AtCSLA2 expression. (*A*) Content of 4-Man and 4-Glc glycosidic linkages in the *Pichia* wall AIR. Values represent percentage of total carbohydrate area detected and show mean + SD of two biological replicates per *Pichia* strain. Vector, empty vector control. (*B*) Hexose sugars enzymatically released from enriched HM polysaccharides. Data show mean + SD of three technical replicates. For each linkage or digestion, different letters indicate significant changes based on one-way ANOVA with post hoc Tukey HSD Test ($P < 0.01$).

The AtMSR1 Protein Is an Optional Cofactor for Glucomannan Synthesis. We designed an in vitro multimer assembly strategy to efficiently integrate two or more transgenes in the *Pichia* genome (*SI Appendix*, Fig. S4 *A* and *B*). We domesticated (removed) the *Pme*I site in the methanol-inducible promoter of the *pPICZ B* vector to create a novel *pPICZ X* vector that was used to clone additional transcriptional units, which can be subsequently fused (*SI Appendix*, Fig. S4*B*). The *Pichia* wall AIR composition was not significantly altered by the expression of *AtMSR1* alone (*SI Appendix*, Fig. S4 *C* and *E*), indicating that this gene is not sufficient for HM production. Interestingly, no *AtMSR1* homolog was identified in *Ak* transcriptome datasets (8, 22). We thus evaluated the function of AtMSR1 in combination with the AkCSLA3 enzyme. Based on monosaccharide and glycosidic linkage analyses, coexpression of AtMSR1 with AkCSLA3 increased the amount of glucomannan in the *Pichia* EM fraction by at least 70% relative to AkCSLA3 alone (Fig. 3 *A* and *B*). The elevated content of EM polysaccharides in the two-gene construct (Fig. 3*A*) did not simply result from changes in *CSLA* gene expression (*SI Appendix*, Fig. S4*E*), nor from changes in HM solubility, as the addition of AtMSR1 also boosted the ability of AkCSLA3 to incorporate 4-Man and 4-Glc into cell wall AIR (*SI Appendix*, Fig. S4*C*). It is noteworthy that AtMSR1 only boosted the content of glucomannan produced by konjac AkCSLA3 without significantly altering its Man:Glc ratio (Fig. 3 and *SI Appendix*, Fig. S4*C*).

AtMSR1 Enables AtCSLA2 to Produce Glucomannan Instead of Mannan. Interestingly, the AtMSR1 cofactor significantly altered the product of AtCSLA2, which is required for glucomannan elongation in *Arabidopsis* (23–25). Glycosidic linkage analysis of wall AIR as well as EM polymers indicated that AtCSLA2 alone produced mannan, but the AtCSLA2 + AtMSR1 *Pichia* strain synthesized glucomannan (Fig. 3*B* and *SI Appendix*, Fig. S4*C* and Table S1). To confirm this structural change, EM polymers were examined with ^{1}H-NMR. The presence of AtMSR1 enabled the AtCSLA2 enzyme to produce both β-1,4-glucosyl- and β-1,4-mannosyl residues instead of pure mannan (Fig. 3*C*). On the basis of the ^{1}H-NMR anomeric signals, the EM polymers contained a 4-Glc to 4-Man ratio of 1:3.2 (Fig. 3*C*), consistent with the 1:3.5–4.5 ratio in the glycosidic linkage analysis (Fig. 3*B*). We performed size-exclusion chromatography to confirm that these glycosyl units are part of the same polymer (i.e., glucomannan), and to investigate its size. EM polymers produced by AkCSLA3 or AtCSLA2, with or without AtMSR1, could only be solubilized by overnight incubation in 10% (wt/vol) sodium hydroxide. Polysaccharides solubilized in this manner were heterodisperse, ranging in size from below 5 kDa to above 270 kDa (Fig. 4*A*). EM

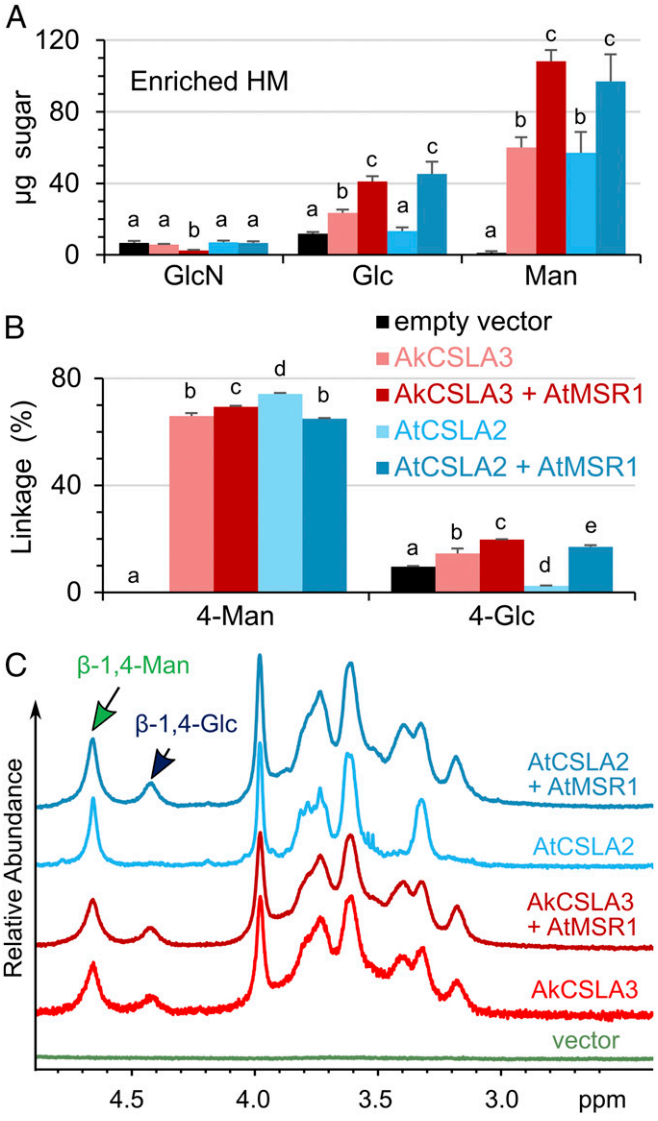

Fig. 3. AtMSR1 is a cofactor for glucomannan synthesis. (*A*) Absolute composition of monosaccharides in EM polymers, enriched from *Pichia* wall AIR. (*B*) Relative content of 4-Man and 4-Glc linkages in the material analyzed in *A*. Values represent molar percentage of total carbohydrates detected. Data show mean + SD of at least three technical replicates. For each sugar or linkage, different letters denote significant changes based on one-way ANOVA with post hoc Tukey HSD Test ($P < 0.05$ for *A*; $P < 0.01$ for *B*). (*C*) ^{1}H-NMR analysis of EM polymers. Arrows indicate diagnostic anomeric peaks.

polysaccharides from three *Pichia* strains (AkCSLA3, AkCSLA3 + AtMSR1, and AtCSLA2 + AtMSR1) were cleaved into fragments smaller than 5 kDa by β-mannanase digestion and contained around 20% Glc (Fig. 4*B*). In contrast, AtCSLA2 alone produced EM polysaccharides that were proportionally smaller (Fig. 4*A*) and contained more than 95% Man (Fig. 4*B*). Only 34% of AtCSLA2 solubilized products were above 50 kDa compared with around 50% of carbohydrates for the three glucomannan-producing strains. In summary, AtMSR1 modulated glucomannan production by AtCSLA2, which increased the content (Fig. 3*A*) and relative size (Fig. 4*A*) of EM polymers isolated from *Pichia* walls.

Influence of MSR1 Proteins on Other Mannan Synthases. We also investigated how AtMSR1 modulates the activity of other mannan synthases such as AtCSLA7, which belongs to a phylogenetic clade distinct from AtCSLA2 (12) and only elongates mannan in vitro (13). Indeed, *Pichia* expressing AtCSLA7 incorporated significantly more 4-Man, but not 4-Glc, linkages into AKI polysaccharides (*SI Appendix*, Fig. S4*D*). In contrast to the AtCSLA2 + AtMSR1 combination (Fig. 3), the coexpression of the *AtMSR1* gene with *AtCSLA7* (*SI Appendix*, Fig. S4*F*) decreased 4-Man production in *Pichia* relative to the single gene controls, without altering the content of 4-Glc in the AKI fraction (*SI Appendix*, Fig. S4*D*).

The *Coffea canephora* (*Cc*) MANS1 mannan synthase represents a prime candidate for the production of mannan in coffee seeds (26), but was inactive when expressed in *Pichia* microsomal membrane fractions and assayed in vitro (27). Unlike AtCSLA2 and AkCSLA3, expression of CcMANS1 alone did not produce any significant amounts of β-1,4-mannan in *Pichia* walls (Fig. 5).

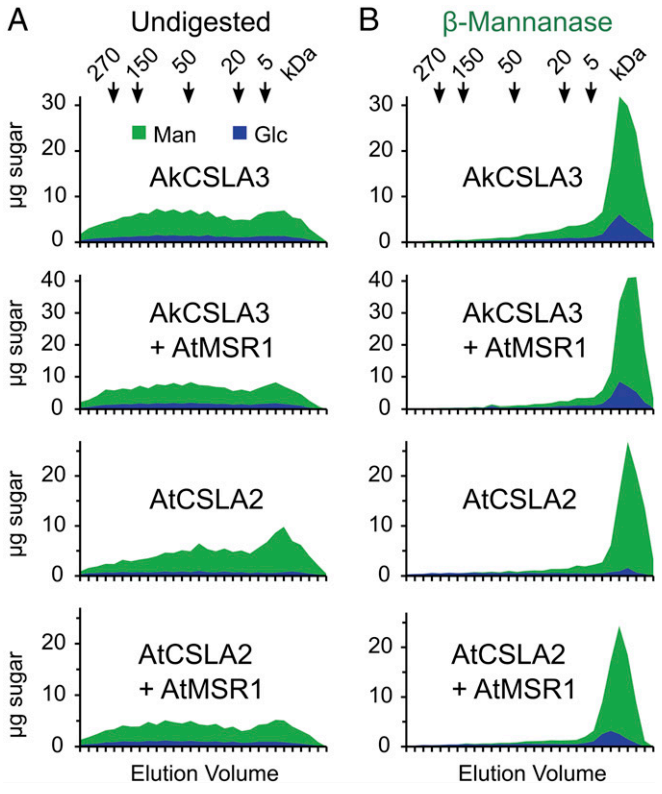

Fig. 4. Size-exclusion chromatography of enriched HM. (*A*) EM polysaccharides were solubilized in 10% NaOH overnight, neutralized, and analyzed by size-exclusion chromatography. Arrows indicate the elution of Dextran standards of known sizes. Data show the Glc and Man content (stacked). (*B*) An equal amount of the EM material used in *A* was digested with β-mannanase before SEC analysis.

Also, coexpression of the *Arabidopsis* AtMSR1 with the coffee CcMANS1 did not produce HM polysaccharides that could be detected via β-mannanase digestion (Fig. 5*A*) or glycosidic linkage analysis of the AKI fraction (Fig. 5*B*). However, coexpression of CcMANS1 with CcMSR1, the cofactor found natively in coffee seeds (26), produced β-1,4-mannan in *Pichia* cells (Fig. 5*A*) without increasing the 4-Glc content of AKI polymers (Fig. 5*B*). Therefore, AtMSR1 enhanced glucomannan synthesis by AtCSLA2 and AkCSLA3, but did not enhance the CcMANS1 and AtCSLA7 mannan synthases. Unlike an auxiliary role of AtMSR1 in glucomannan production by AtCSLA2, we demonstrated that the CcMSR1 protein is an essential cofactor for the synthesis of mannan by the coffee CcMANS1 enzyme.

Functional Characterization of AtMSR1 Conserved Motifs. The AtMSR1 protein has an N-terminal transmembrane (TM) domain and a large PF10250 motif (*SI Appendix*, Fig. S5*A*), which defines a large family of putative GTs in land plants, and has structural similarity to the catalytic domain of protein *O*-fucosyltransferases (PoFUT1) from the animal kingdom (15). Multiple protein alignment pointed to three residues that are conserved in the PF10250 domain of the human (*Homo sapiens*) HsPoFUT1 and MSR-related proteins from *Arabidopsis* (*SI Appendix*, Fig. S5*B*). For example, the AtMSR1 R265 and D355 amino acids correspond to key residues of the HsPoFUT1 sugar-binding motif (*SI Appendix*, Fig. S5*B*). There, the R240 residue is indispensable for HsPoFUT1 catalytic activity, and D340 is within hydrogen-bonding distance of the guanine ring on GDP-fucose (28). Moreover, disulfide bridges contribute to the formation of the PoFUT1 sugar-binding site (29), with the C274 amino acid of AtMSR1 putatively involved in this process (*SI Appendix*, Fig. S5 *A* and *B*). To functionally characterize these motifs, we evaluated how AtMSR1 variants without the TM domain (Δ28) or with missense mutations in three conserved amino acids (R265A, C274A, and D355A) influence HM production by AtCSLA2. Relative to the coexpression of AtCSLA2 with wild-type AtMSR1, the AtMSR1$^{\Delta 28}$ and AtMSR1^{C274A} mutant variants decreased glucomannan production (*SI Appendix*, Fig. S5*C*). The coexpression of AtCSLA2 with mutated AtMSR1 proteins yielded 4-Glc levels similar to the sfGFP control and significantly reduced the 4-Man content relative to the AtCSLA2 + AtMSR1 strain (*SI Appendix*, Fig. S5*D*). Two mutations in AtMSR1 sugar-binding residues impaired glucomannan synthesis by AtCSLA2 to different degrees (*SI Appendix*, Fig. S5 *C* and *D*), and were thus characterized in more detail. Coexpression of AtCSLA2 + AtMSR1^{R265A} not only failed to produce glucomannan but also reduced 4-Man production by more than 50% compared with the AtCSLA2 enzyme alone (Fig. 5). Interestingly, the AtCSLA2 + AtMSR1^{D355A} strain produced HM containing both 4-Man and 4-Glc, albeit at significantly lower levels than the wild-type multimeric construct (Fig. 5). Although less severe than the AtMSR1^{R265A} variant, the addition of AtMSR1^{D355A} still reduced 4-Man accumulation compared with AtCSLA2 expressed alone (Fig. 5*B*). In summary, the AtMSR1 TM domain and sugar-binding motif were important modulators of glucomannan synthesis, and mutations in these regions reduced β-1,4-mannan production by AtCSLA2.

Discussion

Elucidating the mechanisms involved in the synthesis of cell wall polysaccharides remains a challenge in plant biology. Although the genomics era ushered in the identification of multiple genes involved in hemicellulose biosynthesis, many of them remain to be functionally characterized (30). We now demonstrate that yeast synthetic biology tools can be exploited to gain mechanistic insight into HM biosynthesis, which has been difficult to study *in planta* and in vitro. For example, as *Arabidopsis csla7* mutants are embryo-lethal (25), it has previously not been possible to investigate

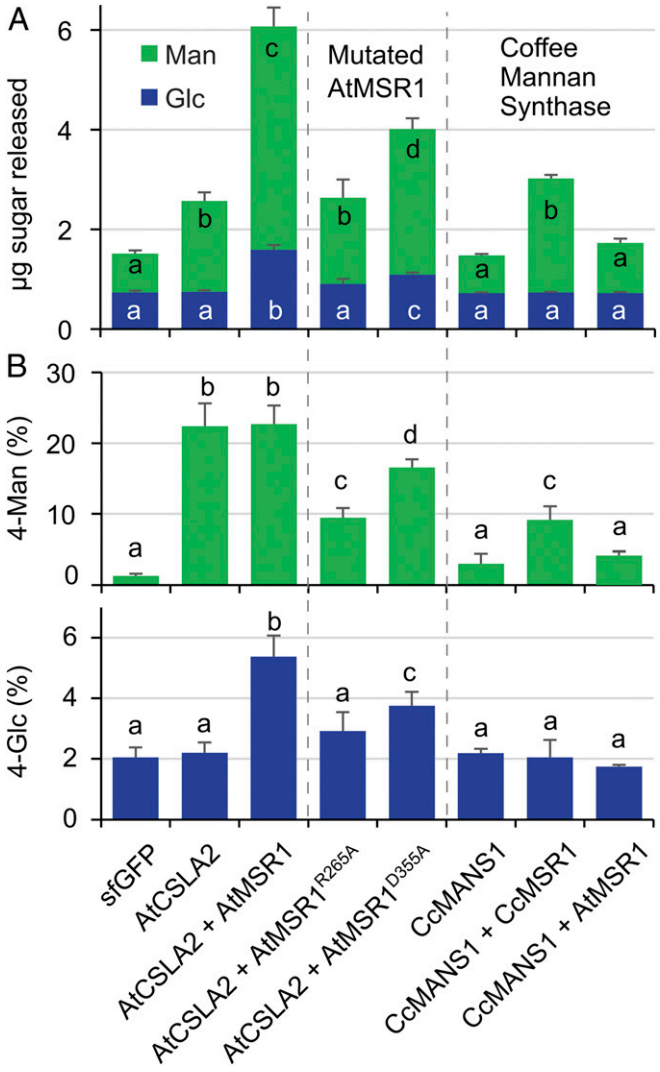

Fig. 5. Importance of MSR1 sugar-binding motif and protein specificity. (*A*) HM sugars released from AKI material digested with β-mannanase. Two point mutations (R265A) and (D355A) were introduced into AtMSR1. CcMANS1, coffee mannan synthase; CcMSR1, coffee MSR1. (*B*) Abundance of 4-Man and 4-Glc in AKI polymers. In all panels, data show mean + SD of three biological replicates. For each glycosyl residue or linkage, different letters denote significant changes based on one-way ANOVA with post hoc Tukey HSD Test ($P < 0.05$).

whether AtCSLA7 functions as a mannan synthase in vivo. In addition to CSLA enzymes, other putative GTs such as MSR proteins were implicated in HM elongation based on plant mutant chemotypes and in vitro assays using plant extracts (15). However, even in heterologous plant hosts, GT activity assays are subject to pleiotropic effects because of the presence of endogenous carbohydrate-related substrates and enzymes. For instance, expression of *Arabidopsis* Cellulose Synthase-Like D 5 (AtCSLD5) or coexpression of AtCSLD2 + AtCSLD3 enhanced mannan synthase activity in tobacco leaves (31, 32). However, AtCSLD3 and AtCSLD5 have also been implicated in cellulose (33) and callose synthesis (34), respectively. GTs required for cell wall biosynthesis have at least one TM domain span, are typically expressed in very low abundance, and are difficult to purify in active form (35). Although in vitro activity assays were previously performed on *Pichia* microsomes containing CSLA proteins (8, 16, 18), these experiments only revealed that the enzymes incorporated exogenous GDP-Man and, to a lesser extent, GDP-Glc into alcohol-insoluble compounds. Because the in vitro assays had limited yields, they relied on [^{14}C]-labeled nucleotide sugar donors. In contrast, we discovered that using only methanol as a carbon source, CSLA-expressing *Pichia* cells produce large amounts of plant HM (Figs. 1*A* and 2 and *SI Appendix*, Fig. S2*D*), which can be structurally characterized in detail using a variety of analytical tools. Because *Pichia* has a fast growth cycle and efficient homologous recombination, it also enables high-throughput studies of genetic permutations of these proteins that are not feasible *in planta* or in vitro.

In this study, we comprehensively analyzed the structures of HM polysaccharides produced by CSLA isoforms from different species. AkCSLA3 expression alone is sufficient for glucomannan production in *Pichia* cells (Fig. 1*A*), which can be enriched up to more than 70% purity in only two steps (Fig. 3*C* and *SI Appendix*, Fig. S3). The enriched HM from the AkCSLA3 yeast strain resembled the structure of konjac glucomannan, its native product (*SI Appendix*, Table S2). Consistent with hemicellulose synthesis in plants (2), AkCSLA3 enzymes were localized in small intracellular punctae in *Pichia*, and their HM products were deposited in the yeast cell wall (Fig. 1 *B* and *C* and *SI Appendix*, Fig. S1 *I* and *J*). Indeed, another (gluco)mannan synthase (AtCSLA9) was previously shown to be Golgi-localized in *Pichia* and had an active site facing the Golgi lumen (18). Thus, *Pichia* likely has endogenous proteins capable of producing and supplying activated GDP-Man and GDP-Glc sugar donors to the CSLA active site. In contrast to AkCSLA3, the expression of two *Arabidopsis* CSLAs yielded relatively pure mannan in *Pichia*. Recombinant AtCSLA2 and AtCSLA7 proteins produced in insect cells were known to have (gluco)mannan and pure mannan synthase activities in vitro, respectively (13). Pointing to diverged roles, AtCSLA2 and AtCSLA9 form a phylogenetic clade distinct from that of the remaining seven CSLA isoforms in *Arabidopsis*, which includes AtCSLA7 (12). Consistent with its lower activity in vitro, AtCSLA7 (*SI Appendix*, Fig. S4*D*) showed reduced mannan production compared with AtCSLA2 in yeast cells (Figs. 2, 3, and 5). However, in contrast to the in vitro study, the AtCSLA2 protein alone did not incorporate significant amounts of 4-Glc in *Pichia*. These observations could be a result of distinct posttranslational modifications of the AtCSLA2 protein and/or the presence of other accessory proteins in *Drosophila* cells that are not present in yeast.

Heterologous expression in yeast enabled us to investigate the roles of MSR accessory proteins in HM biosynthesis, which were previously unclear (15). Although MSR1 proteins alone did not alter *Pichia* wall composition (*SI Appendix*, Figs. S4*C* and S5*C*), they modulated HM synthesis by CSLA enzymes. Potentially, the yeast wall was unchanged after *AtMSR1* expression (*SI Appendix*, Fig. S4 *C* and *E*) because the encoded protein was inactive or unstable in the absence of a CSLA interaction partner. The coffee CcMSR1 was an indispensable cofactor for mannan production by CcMANS1 (Fig. 5). In contrast, AtMSR1 did not enhance the AtCSLA7 (*SI Appendix*, Fig. S4*D*) or the CcMANS1 (Fig. 5) mannan synthases, but was an optional enhancer of glucomannan synthases. The expression of AtMSR1 increased the content of glucomannan produced by AkCSLA3 in *Pichia* (Fig. 3*A* and *SI Appendix*, Fig. S4*C*), without altering its Glc:Man ratio. Furthermore, AtMSR1 enabled AtCSLA2 to produce glucomannan, its expected product in *Arabidopsis* (23–25), instead of mannan (Figs. 3 and 4). Because a single CSLA was sufficient for either glucomannan or mannan synthesis in yeast, MSR proteins are not required to initiate HM elongation. Indeed, *Arabidopsis msr1 msr2* double-mutant plants still contained mannan (15). Therefore, specific MSR cofactors are likely involved in the production of distinct types of HM by modulating CSLA activity. Plant MSR cofactors have sequence homology to mammalian PoFUT1 enzymes, which decorate proteins with O-glycan groups that are essential for cell development (28).

Mutagenesis of three AtMSR1 conserved amino acids, which are involved in nucleotide sugar binding by PoFUT1 enzymes (28, 29), significantly reduced 4-Glc as well as 4-Man incorporation by AtCSLA2 into AKI polymers (Fig. 5 and *SI Appendix*, Fig. S5). Furthermore, the reduced accumulation of HM in the AtCSLA2 + AtMSR1$^{\Delta 28}$ strain (*SI Appendix*, Fig. S5) highlighted the importance of the AtMSR1 membrane-anchoring domain. Although AtMSR1 was an optional modulator of HM synthesis in *Pichia*, the mutated forms tested were detrimental even for the basal activity of the AtCSLA2 enzyme. Because the PoFUT1 sugar-binding motif was structurally conserved and important for the function of AtMSR1 in yeast, we hypothesize that plant MSR proteins may affect CSLA activity via protein glycosylation. Future studies should test this hypothesis by investigating whether CSLA proteins are glycosylated and/or whether they physically interact with the MSR cofactors.

In summary, we established *Pichia* as a convenient biofactory for plant HM production and gained mechanistic insights into mannan and glucomannan production and modulation. This study advances our knowledge of hemicellulose synthesis and also points to other poorly understood aspects that could be resolved using the powerful yeast platform. Furthermore, our approach can be extended to the study of other plant GTs, provided that the appropriate repertoire of substrates is present in yeast, and to investigate how sugar units can be assembled into designer polymers with tailored properties for specific applications.

Methods

Plant genes were cloned and expressed in yeast cells, as recommended by the EasySelect *Pichia* Expression Kit (Invitrogen). After accumulating biomass using glycerol as a carbon source in culture tubes or in multiwell plates (Fig. 5 and *SI Appendix*, Figs. S2, S4, and S5), *Pichia* cells were induced to express recombinant proteins for 24 h, using methanol. For each genotype, at least three independent *Pichia* transformants showed a similar cell wall composition. Polysaccharides isolated from yeast were characterized via glycosidic linkage (36, 37) and monosaccharide analyses (23, 38), as previously described. After enzymatic digestion, solubilized carbohydrates were subjected to monosaccharide analysis, or the anthrone assay (39). *Pichia* cell walls were labeled with specific antibodies according to a protocol previously used for plant seeds (40, 41). Additional details on the protocols used to clone genes, transform and grow *Pichia*, quantify transgene expression, and extract and structurally characterize polysaccharides are presented in the *SI Appendix*, *Materials and Methods*.

ACKNOWLEDGMENTS. We thank Katharina Lufen, Felix Roth, Mara Artz, Caroline Janke, and Ulrike Klauß for technical assistance. We gratefully acknowledge the Center for Advanced Imaging at Heinrich-Heine University for access to the Leica SP8 confocal microscope. The sfGFP vector was kindly provided by Tim Niedzwetzki. This research was supported by Cluster of Excellence on Plant Sciences–Deutsche Forschungsgemeinschaft Grant EXC1028.

1. Pauly M, Keegstra K (2008) Cell-wall carbohydrates and their modification as a resource for biofuels. *Plant J* 54:559–568.
2. Scheller HV, Ulvskov P (2010) Hemicelluloses. *Annu Rev Plant Biol* 61:263–289.
3. Lechat H, Amat M, Mazoyer J, Buleon A, Lahaye M (2000) Structure and distribution of glucomannan and sulfated glucan in the cell walls of the red alga Kappaphycus alvarezii (Gigartinales, Rhodophyta). *J Phycol* 36:891–902.
4. Pauly M, et al. (2013) Hemicellulose biosynthesis. *Planta* 238:627–642.
5. Behera SS, Ray RC (2016) Konjac glucomannan, a promising polysaccharide of Amorphophallus konjac K. Koch in health care. *Int J Biol Macromol* 92:942–956.
6. Bewley JD, Bradford KJ, Hilhorst HWM, Nonogaki H (2013) Structure and composition. Seeds (Springer, New York), pp 1–25.
7. Kuravadi NA, et al. (2013) *Guar: An Industrial Crop from Marginal Farms. Agricultural Sustainability*, eds Bhullar GS, Bhullar NK (Elsevier, London), pp 47–60.
8. Gille S, et al. (2011) Deep sequencing of voodoo lily (Amorphophallus konjac): An approach to identify relevant genes involved in the synthesis of the hemicellulose glucomannan. *Planta* 234:515–526.
9. Buckeridge MS (2010) Seed cell wall storage polysaccharides: Models to understand cell wall biosynthesis and degradation. *Plant Physiol* 154:1017–1023.
10. Willför S, Sundberg A, Hemming J, Holmbom B (2005) Polysaccharides in some industrially important softwood species. *Wood Sci Technol* 39:245–258.
11. Suzuki S, Li L, Sun Y-H, Chiang VL (2006) The cellulose synthase gene superfamily and biochemical functions of xylem-specific cellulose synthase-like genes in Populus trichocarpa. *Plant Physiol* 142:1233–1245.
12. Liepman AH, et al. (2007) Functional genomic analysis supports conservation of function among cellulose synthase-like a gene family members and suggests diverse roles of mannans in plants. *Plant Physiol* 143:1881–1893.
13. Liepman AH, Wilkerson CG, Keegstra K (2005) Expression of cellulose synthase-like (Csl) genes in insect cells reveals that CslA family members encode mannan synthases. *Proc Natl Acad Sci USA* 102:2221–2226.
14. Dhugga KS, et al. (2004) Guar seed beta-mannan synthase is a member of the cellulose synthase super gene family. *Science* 303:363–366.
15. Wang Y, Mortimer JC, Davis J, Dupree P, Keegstra K (2013) Identification of an additional protein involved in mannan biosynthesis. *Plant J* 73:105–117.
16. Wang Y, Alonso AP, Wilkerson CG, Keegstra K (2012) Deep EST profiling of developing fenugreek endosperm to investigate galactomannan biosynthesis and its regulation. *Plant Mol Biol* 79:243–258.
17. Cocuron J-C, et al. (2007) A gene from the cellulose synthase-like C family encodes a beta-1,4 glucan synthase. *Proc Natl Acad Sci USA* 104:8550–8555.
18. Davis J, Brandizzi F, Liepman AH, Keegstra K (2010) Arabidopsis mannan synthase CSLA9 and glucan synthase CSLC4 have opposite orientations in the Golgi membrane. *Plant J* 64:1028–1037.
19. Marcus SE, et al. (2010) Restricted access of proteins to mannan polysaccharides in intact plant cell walls. *Plant J* 64:191–203.
20. Pédelacq JD, Cabantous S, Tran T, Terwilliger TC, Waldo GS (2006) Engineering and characterization of a superfolder green fluorescent protein. *Nat Biotechnol* 24:79–88.
21. Magnelli P, Cipollo JF, Abeijon C (2002) A refined method for the determination of Saccharomyces cerevisiae cell wall composition and beta-1,6-glucan fine structure. *Anal Biochem* 301:136–150.
22. Diao Y, et al. (2014) De novo transcriptome and small RNA analyses of two amorphophallus species. *PLoS One* 9:e95428.
23. Voiniciuc C, et al. (2015) MUCILAGE-RELATED10 produces galactoglucomannan that maintains pectin and cellulose architecture in Arabidopsis seed mucilage. *Plant Physiol* 169:403–420.
24. Yu L, et al. (2014) CELLULOSE SYNTHASE-LIKE A2, a glucomannan synthase, is involved in maintaining adherent mucilage structure in Arabidopsis seed. *Plant Physiol* 164:1842–1856.
25. Goubet F, et al. (2009) Cell wall glucomannan in Arabidopsis is synthesised by CSLA glycosyltransferases, and influences the progression of embryogenesis. *Plant J* 60: 527–538.
26. Joët T, et al. (2014) Regulation of galactomannan biosynthesis in coffee seeds. *J Exp Bot* 65:323–337.
27. Couperthwaite JA (2017) Characterization of CcMANS1, a putative mannan synthase from Coffea canephora. Senior Honors thesis (Eastern Michigan University, Ypsilanti, MI). Available at https://commons.emich.edu/honors/565/. Accessed January 12, 2018.
28. McMillan BJ, et al. (2017) Structure of human POFUT1, its requirement in ligand-independent oncogenic notch signaling, and functional effects of Dowling-Degos mutations. *Glycobiology* 27:777–786.
29. Lira-Navarrete E, et al. (2011) Structural insights into the mechanism of protein O-fucosylation. *PLoS One* 6:e25365.
30. Liepman AH, Wightman R, Geshi N, Turner SR, Scheller HV (2010) Arabidopsis–A powerful model system for plant cell wall research. *Plant J* 61:1107–1121.
31. Verhertbruggen Y, Yin L, Oikawa A, Scheller HV (2011) Mannan synthase activity in the CSLD family. *Plant Signal Behav* 6:1620–1623.
32. Yin L, et al. (2011) The cooperative activities of CSLD2, CSLD3, and CSLD5 are required for normal Arabidopsis development. *Mol Plant* 4:1024–1037.
33. Park S, Szumlanski AL, Gu F, Guo F, Nielsen E (2011) A role for CSLD3 during cell-wall synthesis in apical plasma membranes of tip-growing root-hair cells. *Nat Cell Biol* 13: 973–980.
34. Gu F, et al. (2016) Arabidopsis CSLD5 functions in cell plate formation in a cell cycle-dependent manner. *Plant Cell* 28:1722–1737.
35. Sandhu APS, Randhawa GS, Dhugga KS (2009) Plant cell wall matrix polysaccharide biosynthesis. *Mol Plant* 2:840–850.
36. Ciucanu I, Kerek F (1984) A simple and rapid method for the permethylation of carbohydrates. *Carbohydr Res* 131:209–217.
37. Ciucanu I (2006) Per-O-methylation reaction for structural analysis of carbohydrates by mass spectrometry. *Anal Chim Acta* 576:147–155.
38. Voiniciuc C, Günl M (2016) Analysis of monosaccharides in total mucilage extractable from Arabidopsis seeds. *Bio Protoc* 6:e1801.
39. Foster CE, Martin TM, Pauly M (2010) Comprehensive compositional analysis of plant cell walls (lignocellulosic biomass) part II: Carbohydrates. *J Vis Exp* 37:e1745.
40. Voiniciuc C (2017) Whole-seed immunolabeling of Arabidopsis mucilage polysaccharides. *Bio Protoc* 7:e2323.
41. Voiniciuc C, Günl M, Schmidt MH-W, Usadel B (2015) Highly branched xylan made by IRREGULAR XYLEM14 and MUCILAGE-RELATED21 links mucilage to Arabidopsis seeds. *Plant Physiol* 169:2481–2495.

PNAS
www.pnas.org

Supplementary Information for

Mechanistic Insights from Plant Heteromannan Synthesis in Yeast

Cătălin Voiniciuc, Murali Dama, Niklas Gawenda, Fabian Stritt, and Markus Pauly

Institute for Plant Cell Biology and Biotechnology, Heinrich Heine University, 40225 Düsseldorf, Germany

Corresponding author: Markus Pauly, m.pauly@hhu.de

This PDF file includes:

www.pnas.org/cgi/doi/10.1073/pnas.1814003115

Materials and Methods

Cloning of Plant Genes and *Pichia* Transformation

Plant genes were cloned using the EasySelect *Pichia* Expression Kit (Invitrogen), according to the manufacturer's manual. Full-length cDNA sequences, including their native stop codons, were inserted into the multiple cloning site of *pPICZ B*-based vectors (Invitrogen) and transformed in *E. coli TOP10F'* cells for propagation. The *pPICZ B* vector contains a methanol-inducible *pAOX1* promoter for recombinant protein expression and a constitutively expressed marker for Zeocin selection in bacteria and yeast (Fig. S4*A*). The following transcripts were amplified using the primers listed in Supplemental Table S3 from their native tissues: *AkCSLA3* (GenBank: ADW77641.1) from the developing konjac corm (1), *AtCSLA2*, *AtMSR1* and *AtCSLA7* from developing Arabidopsis siliques (2). For *AtCSLA7*, "GCT" was added following the native start codon to ensure efficient translation initiation in yeast. The coffee *CcMANS1* and *CcMSR1* were synthesized in a codon-optimized form for *Pichia* expression (GeneArt), and without the restriction sites present in the *pPICZ B* vector. Multimeric gene constructs were assembled *in vitro* using an enhanced version of the method described in the Multi-Copy Pichia Expression Kit manual (Invitrogen). The *Pme*I site in *pAOX1* was domesticated (removed) using the Phusion Site-Directed Mutagenesis Kit (Thermo Fisher Scientific) to yield a *pPICZ X* vector (Fig. S4*B*), which was used to clone *MSR* genes. Additional site-directed mutagenesis experiments (including domestication of *BamH*I site in *AtCSLA7*) were performed using the same kit, and the primers listed in Table S3. Each *MSR* transcriptional unit, flanked by unique *Bgl*II and *BamH*I sites, was cut from *pPICZ X* and inserted into the *BamH*I site of a *pPICZ B* + *CSLA* vector (Fig. S4*B*).

Constructs were verified by colony PCR and Sanger sequencing using the vector- and gene-specific primers listed in Table S3. Transgenes were integrated into the *pAOX1* region of the *Pichia pastoris* X-33 genome via homologous recombination. *Pichia* cells were transformed via the condensed protocol (3), using 150 ng of linearized plasmid DNA. At least three independent *Pichia* colonies containing the desired transgene(s) were identified by genotyping using *pPICZ* vector and insert-specific primer combinations that would produce unique amplicons (Table S3).

Pichia Growth and Cell Wall Isolation

For each construct, cells from at least three independent *Pichia* transformants were grown in buffered glycerol-complex medium (BMGY) to accumulate biomass, and were then induced to express recombinant proteins for 24 h using buffered methanol-complex medium (BMMY), as described in the EasySelect *Pichia* Expression Kit (Invitrogen). Cells were grown at 30°C and 225 rpm, in 14 mL culture tubes or in 24-well plates (Fig. 5, Fig. S1*B*, Fig. S2, Fig. S4 and Fig. S5). In culture tubes, cells were grown overnight in 2 to 3 mL of BMGY, collected by centrifugation (2000 *g* for 2 min), and re-suspended in an equal volume of BMMY. To compare more strains in parallel, *Pichia* was cultured in multi-well plates as previously described (4), with minor modifications. Cells were grown in 600 µL of BMGY for around 60 h, which leads to glycerol depletion (4), and then the *pAOX1* promoter was induced by the addition of 600 µL of BMMY2 (4), containing 1% methanol (twice as much as in the regular BMMY medium).

After methanol induction, *Pichia* cells were transferred to 2 mL tubes and collected by centrifugation. For wall AIR isolation, cells were mechanically lysed with 1 mL of ethanol and glass beads (Sigma, Catalog number G8772) for 2:30 min at 30 Hz using a ball mill (Retsch Mill MM400). After centrifugation for 2 min at 10000 *g*, the supernatant was discarded and the pellet was washed further with 1 mL of chloroform:methanol (1:1 v/v), and finally with 1 mL of acetone. The resulting AIR material was dried, and directly used for carbohydrate analysis or for enrichment of HM polysaccharides. For Fig. S1*B*, glycans in 600 µL of the BMMY supernatant

(after pelleting cells) were precipitated with 1.4 mL of ethanol, and washed as described for the wall AIR material.

Enrichment of HM Polysaccharides

Mannosylated proteins were extracted from *Pichia* wall material with 1 M NaOH for 60 min at 75°C and 1400 rpm in a thermomixer (Eppendorf), as previously described (5). After neutralizing the solution with acetic acid, AKI polymers were pelleted at 20000 *g* for 2 min and washed with water to remove the alkaline-soluble carbohydrates. The resulting AKI material was resuspended in 600 µL of water by mixing at 30 Hz for 2:30 min using a ball mill, and used immediately for enzymatic digestion or stored at 4°C.

Yeast β-1,3-glucans were enzymatically removed from *Pichia* AKI material as previously described (5). Samples were mixed for 2 days at 37°C with at least 1 mg of Zymolyase 20T from *Arthrobactor luteus* (USBiological), in 100 mM potassium phosphate buffer (pH 7.0), containing sodium azide as a preservative. The resulting EM polysaccharides, which remain insoluble, were then washed twice with water.

Structural Analysis of Polysaccharides

Glycosidic linkages in *Pichia* material were analyzed by gas chromatography–mass spectrometry following derivatization of partially methylated alditol acetates as described (6), with modifications by (7). Carbohydrates were separated using a 5977A Series GC-MS system (Agilent) equipped with a SP-2380 capillary column (Supelco). Carbohydrate peaks were annotated based on their retention time and ion spectra relative to standards.

Monosaccharide composition was analyzed via high-performance anion-exchange chromatography coupled with pulsed electrochemical detection (HPAEC-PAD), as previously described (2, 8), on a 940 Professional IC Vario ONE/ChS/PP/LPG instrument (Metrohm) equipped with CarboPac PA20 guard and analytical columns.

For enzymatic characterization, AKI or EM polymers were incubated with 1 U of endo-1,4-β-Mannanase (Megazyme, E-BMABC) or Cellulase (Megazyme, E-CELBA) for 30 min at 40°C and 1000 rpm in a thermomixer (Eppendorf). Afterwards, the samples were centrifuged for 2 min at 20000 *g*, and 100 uL of the supernatant was used to quantify for the amount of sugar release. Total hexose sugars were quantified using the anthrone assay (9), and the monosaccharide composition of the solubilized material was determined by HPAEC-PAD.

For ^{1}H-NMR analysis, enriched HM polysaccharides were dissolved in 0.3 mL of 10% NaOD / D_2O solution (99.9% atom D), containing 0.05% (w/w) of 3-(trimethylsilyl)-propionic-2,2,3,3-d4 acid sodium salt. The ivory nut mannan, konjac glucomannan, yeast β-glucans, curdlan (all from Megazyme), cellopentaose, and cellulose (both from Sigma–Aldrich) standards were dissolved as described for the *Pichia* samples. The ^{1}H-NMR spectra were recorded on a Varian 400 MHz NMR spectrometer equipped with a ^{1}H/^{13}C probe at 298 K. All chemical shifts were referenced relative to 3-(trimethylsilyl) propionic-2,2,3,3-d4 acid (0.00 ppm for ^{1}H). The NMR data was processed and analyzed using Bruker's Topspin 3.5 software.

Prior to SEC analysis, EM polymers were incubated for 16 h in 10% NaOH at 60°C and 1400 rpm in a thermomixer (Eppendorf). The material was then mixed for 10 min at 30 Hz using a ball mill, neutralized with acetic acid, and sonicated for a total of 120 min at 80°C (vortex mixing every 30 min). After centrifugation for 10 min at 10000 *g* the amount of polysaccharides in the supernatant was quantified with the anthrone assay. Solubilized EM polymers (180 to 300 µg) were injected into an NGC Quest 10 Plus Chromatography System (Bio-Rad) equipped with a Tricorn Superose 6 column (GE Healthcare) and a refractive index detector (RID 20A, Shimadzu). Water was used as a mobile phase, and an equal amount of each sample was also injected after digestion with 10 U of endo-1,4-β-mannanase (Megazyme, E-BMABC) for 30 min

at 40°C and 1000 rpm. Dextran standards of known molecular size were subjected to SEC similar to the *Pichia* samples.

Fluorescent Imaging of *Pichia* Cells

Polysaccharides in *Pichia* cell walls were labelled using a protocol previously used for plant seeds (10, 11) with modifications. After 24 h of methanol induction, 100 µL of *Pichia* cells were pelleted by centrifugation at 400 *g* for 2 min. Cells were resuspended in 100 µL of phosphate-buffered saline (PBS), pH 7.0 solution. After adding 0.6 µL of 2-mercaptoethanol and 1 µL of Zymolyase 20T (125 µg), cells were incubated for 20 min at 30°C, 1000 rpm in a thermomixer (Eppendorf) to partially remove native yeast polymers. The cells were pelleted and washed with PBS, before sequentially incubating them in antibody solutions as previously described (10). The LM21 and LM22 primary antibodies (PlantProbes, www.plantprobes.net), which are directed against HM polysaccharides (12), were diluted 1:5, while Goat anti-Rat IgG Alexa Fluor 488 (Invitrogen) secondary antibody was diluted 1:50. Native polysaccharides in the yeast wall were counterstained with 1% (w/v) calcofluor white for 60 min, and then rinsed well with PBS.

The plasma membrane of cells expressing sfGFP or sfGFP-AkCSLA3 proteins was stained with the FM4-64 dye (Invitrogen) immediately before imaging, as previously described (13).

Fluorescent signals were acquired with a Leica DM2000 microscope equipped with pE-300 white (CoolLED) illumination and an L5 filter cube (Leica), or with a Leica TCS SP8 STED 3X confocal system. On the Leica SP8 system, the following parameters were used to detect the different fluorophores: calcofluor (405 nm excitation, 405 to 450 nm emission); sfGFP and Alexafluor 488 (488 nm excitation, 500 to 530 nm emission); FM4-64 (552 nm excitation, 590 to 700 nm emission). For each experiment, images were processed uniformly using the Fiji software (14).

Quantitative reverse transcription PCR (RT-qPCR)

Pichia cells were grown in the 24-well plate format described above. After 24 h of methanol induction, 150 uL of cells were transferred to new tubes for RNA extraction, and the rest of the cell culture was used for wall carbohydrate analysis. Total RNA was isolated using the YeaStar RNA Kit (Zymo, R1002), according to the manufacturer's instructions, including on-column digestion with DNase I Set (Zymo, E1010). The eluted RNA was used immediately or stored at -80ºC. To remove any remaining DNA contamination, at least 1 µg of eluted RNA was further treated with DNase I in a new tube and purified using the RNA Clean & Concentrator™-5. The final concentration and purity of nucleic acids was measured using the Eppendorf BioSpectrometer, and Qubit dsDNA and RNA high sensitive kits. First-strand cDNA was synthesized from 200 ng of RNA using the iScript kit (BioRad, 170-8891).

RT-qPCR was performed on a MyiQ system using iQ SYBR Green Supermix (BioRad), according to manufacturer's protocol. Each 20 µL reaction contained 300 nM of F and R primers and 0.2 µL of first-strand cDNA. Negative controls with only RNA were also tested for each sample. The primers used for the RT-qPCR experiment are listed in Table S4. *Pichia ARG4*, argininosuccinate lyase (15) and *TAF10*, subunit of Transcription initiation factor TFIID (16), were previously validated as reference genes. Fold change gene expression, normalized to the geometric mean of *Pichia ARG4* and *TAF10*, was calculated using the Pfaffl method (17, 18).

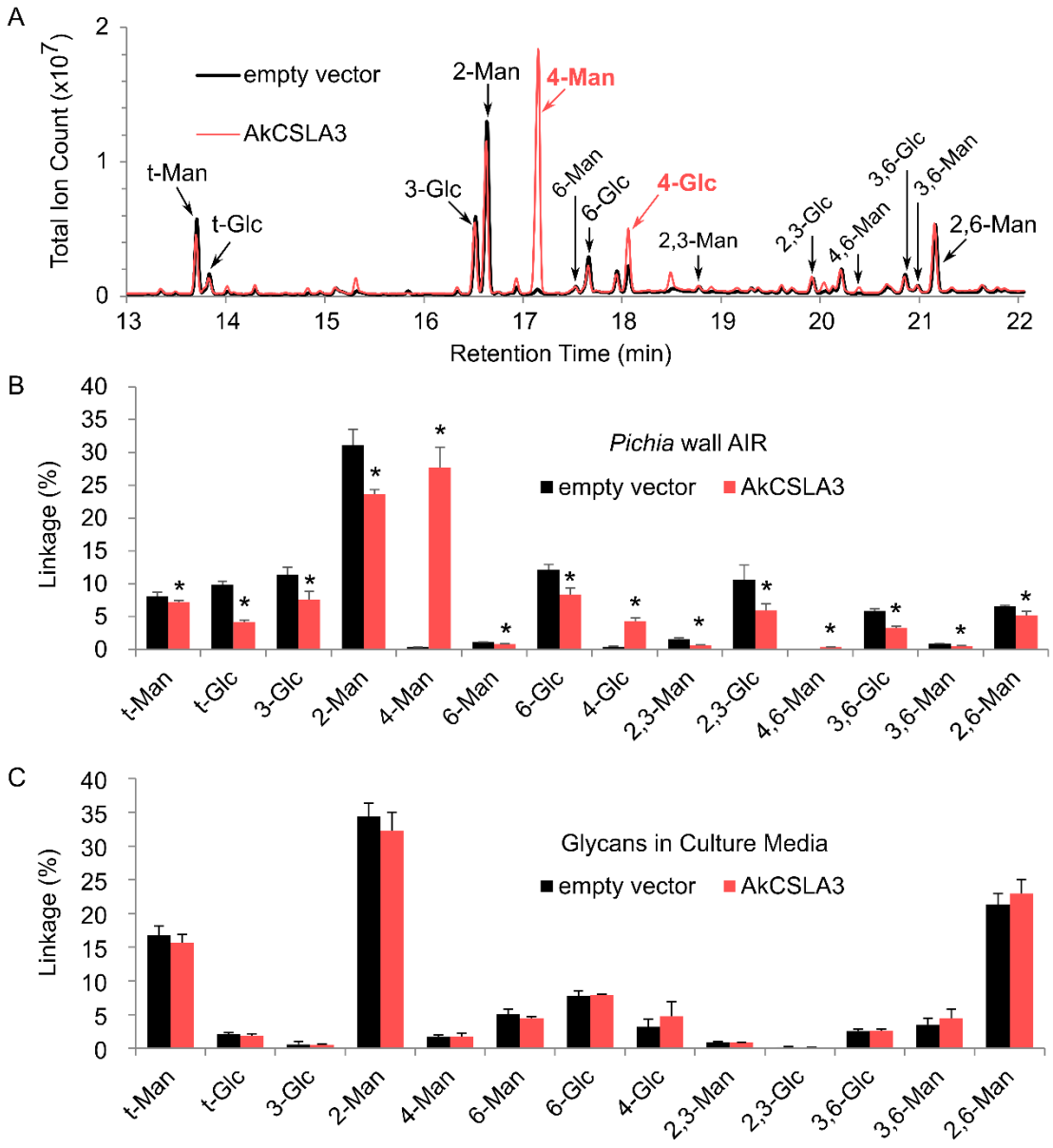

Fig. S1. Analysis of polysaccharides in *Pichia* cells and growth media. (*A*) GC-MS chromatogram of the cell wall glycosidic linkages (quantified in Fig. 1) produced by the empty vector control and the konjac AkCSLA3. Non-labelled peaks could not be assigned to carbohydrate derivatives. (*B*) Linkage composition of the cell wall alcohol-insoluble residue (AIR). Data show mean + SD of 6 independent transformants for each genotype. (*C*) Linkage composition of the ethanol-precipitable glycans secreted into the culture media by *Pichia* cells. Data show mean + SD of 3 biological replicates. In (*B*) and (*C*), asterisks mark significant changes between the empty vector control and AkCSLA3 strain (two-tailed *t*-test, $P < 0.05$).

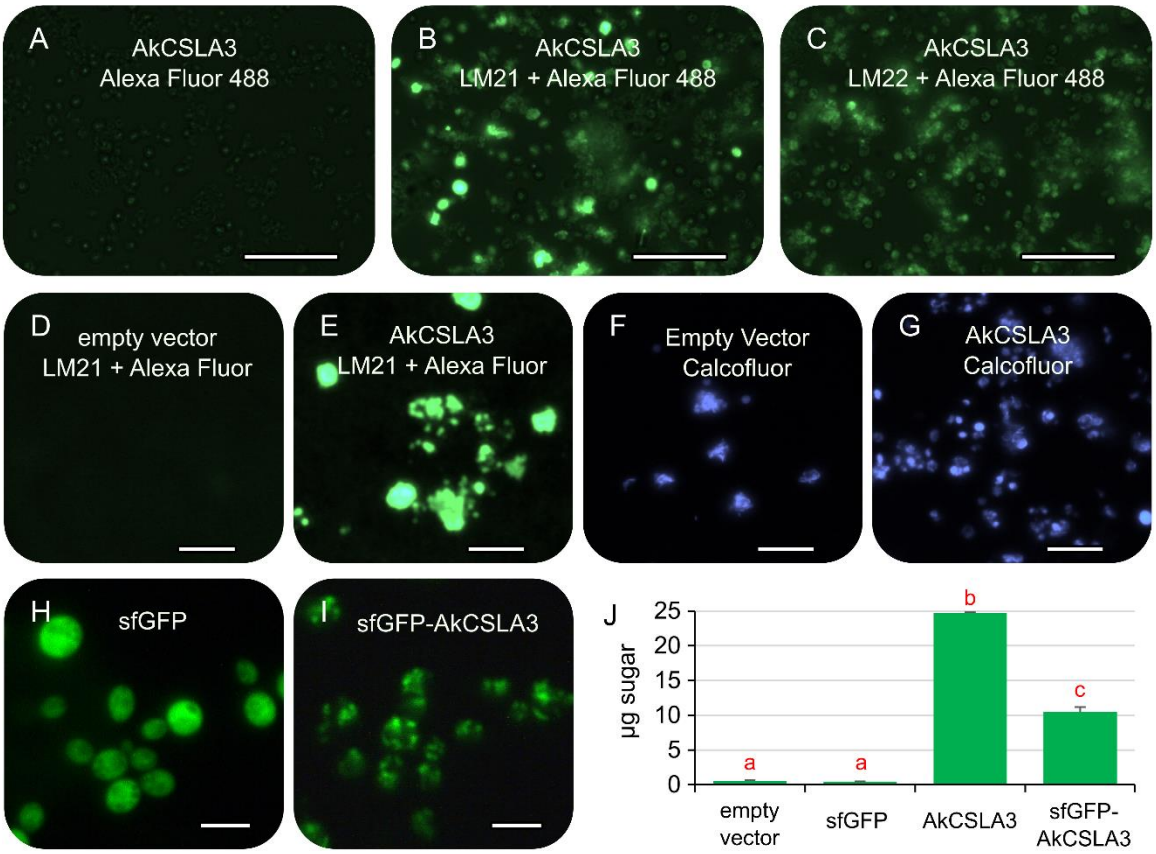

Fig. S2. Imaging of polysaccharides in the *Pichia* cells. (*A*) Yeast cells expressing AkCSLA3 immunolabeled without a primary antibody. (*B*) LM21 and (*C*) LM22 immunolabeling of the AkCSLA3 cells. (*D*) and (*E*) LM21 labelling on empty vector strain and AkCSLA3 expressing strain. (*F*) and (*G*) Calcofluor labelling of both *Pichia* strains. (*H*) and (*I*) Imaging of Pichia cells expressing super folder green fluorescent protein (sfGFP) or sfGFP-tagged AkCSLA3, respectively. (*J*) Amount of sugar released by β-1,4-mannanase from enriched HM polysaccharides extracted from *Pichia* cells (see Fig. S3 for details) imaged in panels (*H*) and (*I*). Data show mean + SD of 3 technical replicates. Different letters indicate significant changes based on one-way ANOVA with post-hoc Tukey HSD Test ($P<0.01$). (Scale bars: *A* to *C*, 50 µm; *D* to *I*, 10 µm).

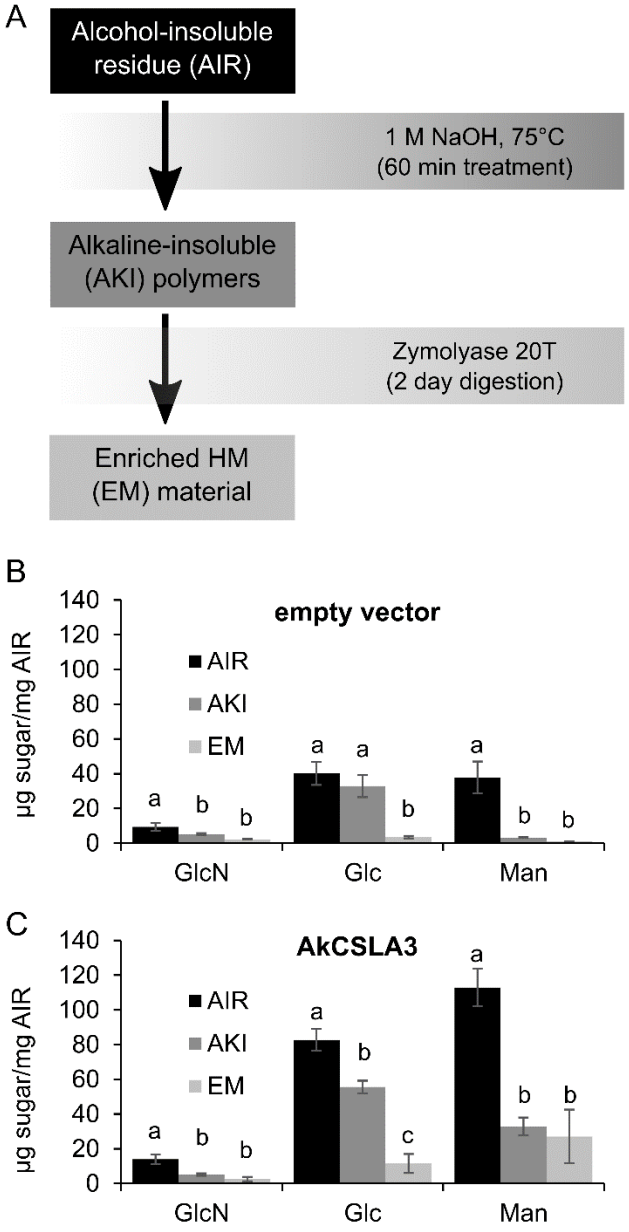

Fig. S3. Chemical and enzymatic enrichment of HM polymers from the *Pichia* cell wall. (*A*) Strategy for enriching HM polysaccharides from *Pichia* wall AIR. (*B*) and (*C*) Monosaccharide composition of AIR material, and sequentially isolated AKI and EM fractions from empty vector and AkCSLA3 strains, respectively. Data show the mean ± SD of 3 biological replicates. Glucosamine (GlcN) is derived from yeast chitin. For each sugar in panels (*B*) and (*C*), distinct letters indicate significant changes between different wall fractions based on one-way ANOVA with post-hoc Tukey HSD Test ($P < 0.01$).

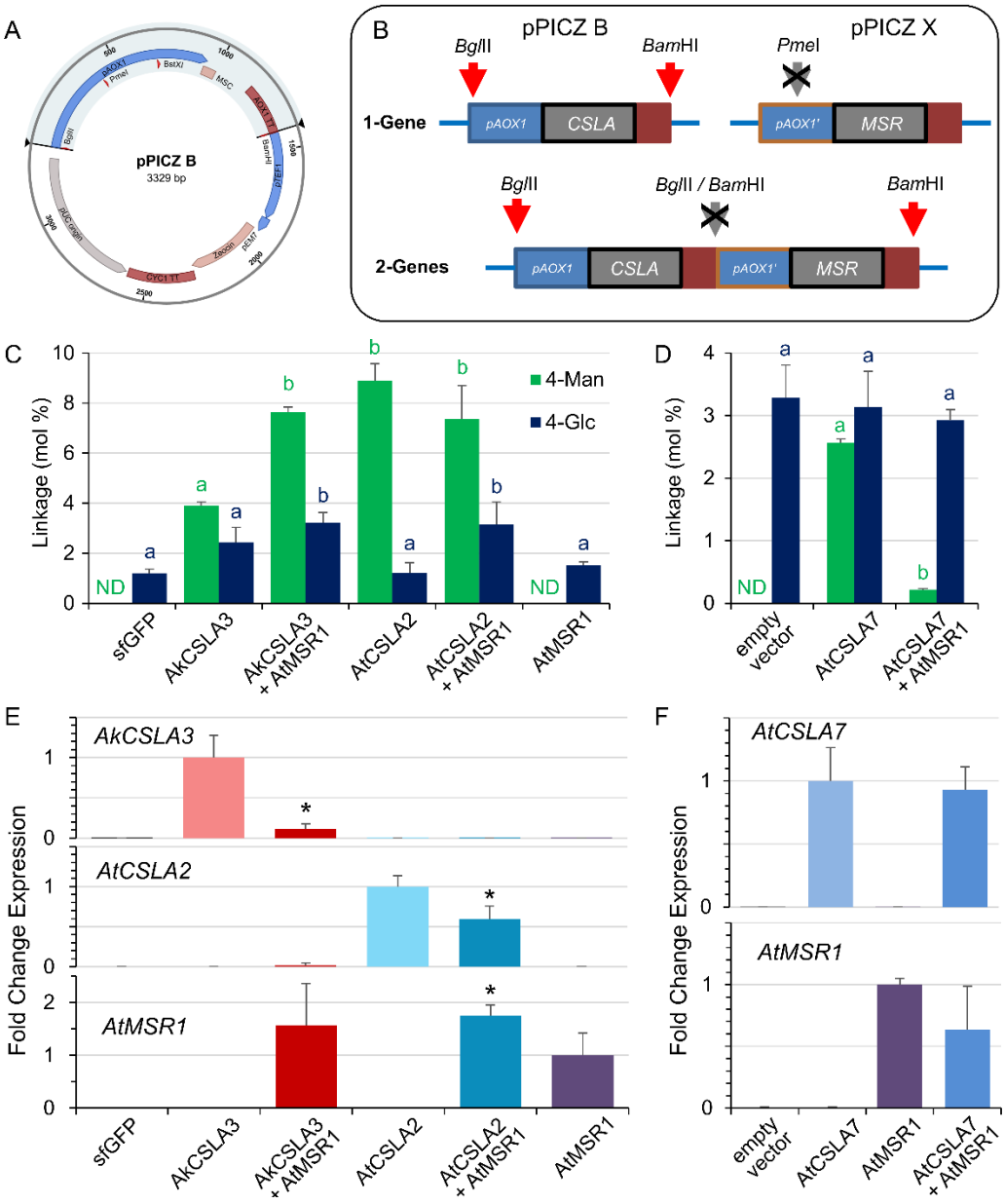

Fig. S4. *Pichia* multimeric gene constructs. (*A*) Graphic map of the pPICZ B vector. The *Bgl*II-*Bam*HI cassette contains a full transcriptional unit. (*B*) The *Pme*I site in the pPICZ B vector was removed to produce the pPICZ X entry vector. Two distinct transcriptional units cloned in the pPICZ B and pPICZ X vectors can be joined using *Bgl*II / *Bam*HI complementary ends. (*C*) Glycosyl linkage analysis of *Pichia* wall AIR. (*D*) Glycosyl linkage analysis of AKI polymers. Values represent the molar percentage of total carbohydrate linkages detected, and show mean + SD of 3 biological replicates (only 2 for AtCSLA7 and AtCSLA7 + AtMSR1). For each linkage, distinct letters indicate significant changes in one-way ANOVA with post-hoc Tukey HSD Test ($P < 0.05$). (*E*) and (*F*) Transcript levels quantified with RT-qPCR. The expression of each gene of interest was normalized to *Pichia ARG4* and *TAF10* reference genes and set as 1.0 in the respective single gene strain. Data show mean + SD of three biological replicates. Asterisks mark a significant change relative to the respective single gene strain (two-tailed *t*-test, $P < 0.05$).

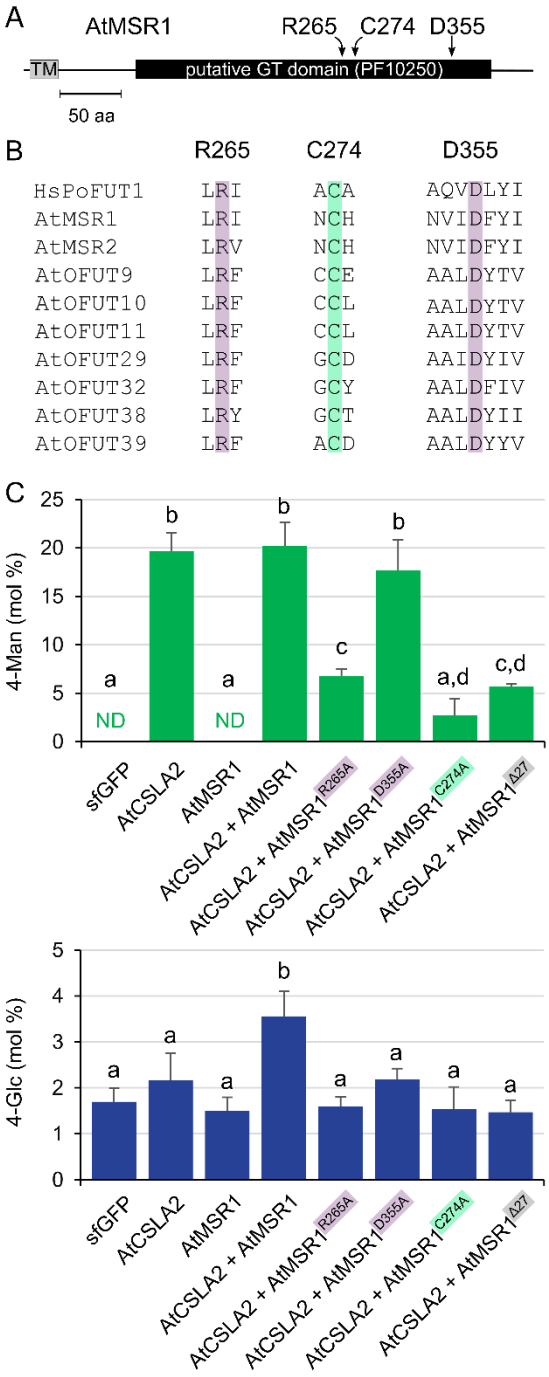

Fig. S5. Characterization of conserved AtMSR1 amino acids. (*A*) Features of the AtMSR1 protein, including conserved residues. TM – transmembrane domain. (*B*) Alignment of AtMSR1 and related Arabidopsis proteins to the human protein o-fucosyltransferase1 (HsPoFUT1), showing three conserved amino acids. (*C*) Effect of missense mutations and TM deletion (Δ27) on AtMSR1 function. Abundance of 4-Man and 4-Glc linkages in AKI polymers, as a molar percentage of total carbohydrates detected. Data show mean + SD of 3 biological replicates. ND, not detected. Distinct letters indicate significant changes in one-way ANOVA with post-hoc Tukey HSD Test ($P < 0.05$).

Table S1. Glycosidic linkage composition of HM produced in *Pichia*. Table shows the full dataset for the enriched mannan (EM) material analyzed in Fig. 3*C*. Values represent molar percentage of total carbohydrates detected. "Others" include trace amounts of 3,6-Man and 2,6-Man linkages. Data show mean ± SD of 4 technical replicates.

	empty vector	**AkCSLA3**	**AkCSLA3 + AtMSR1**	**AtCSLA2**	**AtCSLA2 + AtMSR1**
t-Man	1.7 ± 0.2	3.0 ± 0.6	1.6 ± 0.2	2.6 ± 0.2	1.3 ± 0.1
t-Glc	10.6 ± 0.4	2.9 ± 0.3	2.0 ± 0.3	2.3 ± 0.0	2.6 ± 0.0
3-Glc	4.6 ± 0.1	0.9 ± 0.1	0.5 ± 0.1	0.8 ± 0.0	0.7 ± 0.0
2-Man	3.9 ± 0.2	1.5 ± 0.2	0.8 ± 0.1	2.2 ± 0.1	1.0 ± 0.1
4-Man	0.0 ± 0.0	66.0 ± 1.0	69.4 ± 0.3	74.2 ± 0.4	64.9 ± 0.3
6-Glc	51.4 ± 0.4	8.2 ± 1.3	4.6 ± 0.2	10.8 ± 0.1	9.4 ± 0.5
4-Glc	9.6 ± 0.2	14.5 ± 1.8	19.7 ± 0.2	2.5 ± 0.1	17.0 ± 0.6
3,6-Glc	14.8 ± 0.4	1.7 ± 0.4	0.6 ± 0.1	2.8 ± 0.0	2.1 ± 0.1
Others	3.4 ± 0.4	1.4 ± 0.2	0.8 ± 0.0	1.9 ± 0.1	1.1 ± 0.1

Table S2. Peaks in the ^{1}H-NMR spectra of HM produced in *Pichia*.
Standard polysaccharides and enriched mannan (EM) material from *Pichia* were analyzed using similar conditions. The data represent chemical shifts (ppm) of each peak. EM material from the empty vector control did not show any carbohydrate peaks. *Pichia* strains expressing *Arabidopsis thaliana* CSLA2 (AtCSLA2) or *Amorphophallus konjac* CSLA3 (AkCSLA3) were examined in two independent experiments (Exp 1 and Exp 2).

Polymer / *Pichia* Strain	H1	H2	H3	H4	H5	H6a	H6b
Mannan	4.67	4.04	3.70	3.80	3.42	3.70	3.85
Glucomannan							
β-1,4-mannan	4.68	4.04	3.70	3.80	3.42	3.70	3.85
β-1,4-glucan	4.46	3.29	3.44-3.62	3.44-3.62	3.44-3.62	3.73-3.91	3.73-3.91
Cellopentose	4.46	3.29	3.53	3.53	3.53	3.91	3.76
Yeast β-glucans							
β-1,3-glucan	4.70	3.46	3.61	3.39	3.39	3.92	3.61
β-1,6-glucan	4.42					4.29	
Curdlan	4.70	3.46	3.61	3.39	3.39	3.92	3.61
Exp 1 – AtCSLA2 (mannan**)**	4.68	4.04	3.70	3.80	3.42	3.70	3.85
Exp 1 – AkCSLA3							
β-1,4-mannan	4.67	4.04	3.70	3.80	3.42	3.70	3.85
β-1,4-glucan	4.46	3.30	3.44-3.62	3.44-3.62	3.44-3.62	3.73-3.91	3.73-3.91
Exp 2 – AkCSLA3							
β-1,4-mannan	4.67	4.04	3.70	3.80	3.42	3.70	3.85
β-1,4-glucan	4.46	3.29	3.44-3.62	3.44-3.62	3.44-3.62	3.73-3.91	3.73-3.91
Exp 2 – AkCSLA3 + AtMSR1							
β-1,4-mannan	4.67	4.04	3.70	3.80	3.42	3.70	3.85
β-1,4-glucan	4.46	3.29	3.44-3.62	3.44-3.62	3.44-3.62	3.85	3.85
Exp 2 – AtCSLA2 (mannan)	4.67	4.04	3.70	3.80	3.42	3.73-3.91	3.73-3.91
Exp 2 – AtCSLA2 + AtMSR1							
β-1,4-mannan	4.67	4.04	3.70	3.80	3.42	3.70	3.85
β-1,4-glucan	4.46	3.29	3.44-3.62	3.44-3.62	3.44-3.62	3.73-3.91	3.73-3.91

Table S3. Sequences of primers used for cloning, genotyping and sequencing. Primers are sorted based on their primary purpose. F or R denote the forward or reverse orientation. Introduced restriction sites are marked in bold, and modified bases are in red.

	Primer Target and Direction	5' to 3' Sequence
cDNA cloning	AkCSLA3 (ATG to TAG) F	atc**TTCGAA**ATGGCCATCGACTGG
	AkCSLA3 (ATG to TAG) R	tga**CACGTG**CTACTTTTCACTAGGAACAAAGG
	AtCSLA2 (ATG to TAG + 8 bp of 3' UTR) F	gta**TTCGAA**ATGGACGGTGTATCACCAAAG
	AtCSLA2 (ATG to TAG + 8 bp of 3' UTR) R	aat**CACGTG**CACAACTACTAACTCGGGACATAAG
	AtMSR1 (ATG to TGA) F	ga**TTCGAA**ATGGGTGTTGATTTGAGGCA
	AtMSR1 (ATG to TGA) R	gtt**CACGTG**TCAGCAAAAGCATGAATAAGCC
	AtCSLA7 (ATG, + gtc, to TAG) F	ta**CACGTG**atATGgctTCTCCTCTCCCAATCTTCC
	AtCSLA7 (ATG, + gtc, to TAG) R	gcctgttt**CACGTG**CTATGCTAAGTAAGAGGAAGCAGG
Sequencing + Genotyping	pPICZ primer F	GACTGGTTCCAATTGACAAGC
	pPICZ primer R	GCAAATGGCATTCTGACATCC
	AkCSLA3 R	TATTGCCATCTTCCTCACCAG
	AkCSLA3 F	GAGCAGGAGTCAGGCTCATC
	AtCSLA2 F	CGCCGGAATATGGAGAATAG
	pPICZ 3' end of pUC origin F	CTTTTCTACGGGGTCTGACG
	pPICZ B cloning site R	CACGTGAATTCCTCGTTTCG
	AtMSR1 R	ACAGGATCAGTTTCGCCATC
	AtMSR1 F	GGTGGCTAAGCATCTTGGAG
	AtCSLA7 R	GAACCCAAAGAAGGCAAATG
	AtCSLA7 F	TCCAGCCAGTAAGGAGTTGG
	CcMANS1 R	CGACGATTTTACGGACGAAG
	CcMANS1 F	AGAGTTGGCTTTGGTTCAGG
	CcMSR1 R	AGGATTCGTGCCATTCAGTC
	CcMSR1 F	TTCCTTGGACGGTGTTATCC
Site-Directed Mutagenesis	pPICZ B (no PmeI, 2 bp del) F	aaacgctgtcttggaacctaatatg
	pPICZ B (no PmeI, 2 bp del) R	actgtcagttttgggccatttg
	AtCSLA7 (no BamHI) F	ATGATTCCACGGAcCCAGCCAGTAA
	AtCSLA7 (no BamHI) R	CAAGCACTTGAATTATTATACGATTCGATGGC
	AtMSR1 (R265A) F	CATAGCAGTAGACCTTgcAATCGACATACTTG
	AtMSR1 (R265A) R	AAACGGCCACCGGATTTACGG
	AtMSR1 (D355A) F	GCTTATGTAGAAagCGATAACATTTTCGTACTCGG
	AtMSR1 (D355A) R	TCAAGAAGCGATGTCTTTGTTCCAGC
	AtMSR1 (C274A) F	GAGAAGAAAAATgctCATACAACTGGTGTAGTAGGG
	AtMSR1 (C274A) R	AAGTATGTCGATTCTAAGGTCTACTGCTATGAAACGG
	AtMSR1 (Δ27) F	gccTTCGAAATGGATTACTTTGATTCTCTTCAGGAG
	AtMSR1 (Δ27) R	gttCACGTGTCAGCAAAAGCATGAATAAGCC
Genotyping	pPICZ X mutated PmeI region F	TGACAGAAACGCTGTCTTGG
	AtCSLA2 multimer F	CAATGTCTTTCTTCATCAGTGG
	start of AtMSR1 R	AGCATCTGTCCAAGCATCAC
	binds start of CcMSR1 R	TCAGGATAGCAGCAACAACC
	binds end of CcMANS1 F	AGGCTGGTGCCTTCTTCAC

Table S4. Sequences of primers used for RT-qPCR.
For each primer, F or R indicates its orientation and the third column lists the sequence source.

Primer Target and Direction	5' to 3' Sequence	Design Tool / Reference
Pichia ARG4 F	TCCTCCGGTGGCAGTTCTT	Primer-BLAST (19)
Pichia ARG4 R	TCCATTGACTCCCGTTTTGAG	published sequence (15)
Pichia TAF10 F	ATTGAGGAAGAGCCCGAACC	published sequence (15)
Pichia TAF10 R	GCGTGAATTCTTCGTCCTCC	Primer-BLAST (19)
AkCSLA3 F	TGCATCTCCCGACAACCATC	Primer-BLAST (19)
AkCSLA3 R	TCCCGATCTCCAACAAACCG	Primer-BLAST (19)
AtCSLA2 F	TTGCGGCTTTCTTGTTCGTG	Primer-BLAST (19)
AtCSLA2 R	CATAAGTCCCGATCCAGCCC	Primer-BLAST (19)
AtMSR1 F	ATGACGCTGTATCATCGAAAGGG	Primer-BLAST (19)
AtMSR1 R	GCCACCATTACAGCATCAGTG	Primer-BLAST (19)
AtCSLA7 F	AAAGGCTCTGGTCATGGGCTTG	QuantPrime (20)
AtCSLA7 R	TAGCTCCAGCAAATGCACCCTCTC	QuantPrime (20)

References

1. Gille S, et al. (2011) Deep sequencing of voodoo lily (Amorphophallus konjac): An approach to identify relevant genes involved in the synthesis of the hemicellulose glucomannan. *Planta* 234:515–526.
2. Voiniciuc C, et al. (2015) MUCILAGE-RELATED10 Produces Galactoglucomannan That Maintains Pectin and Cellulose Architecture in Arabidopsis Seed Mucilage. *Plant Physiol* 169(1):403–420.
3. Lin-Cereghino J, et al. (2005) Condensed protocol for competent cell preparation and transformation of the methylotrophic yeast Pichia pastoris. *Biotechniques* 38(1):44–48.
4. Weis R, et al. (2004) Reliable high-throughput screening with Pichia pastoris by limiting yeast cell death phenomena. *FEMS Yeast Res* 5(2):179–189.
5. Magnelli P, Cipollo JF, Abeijon C (2002) A refined method for the determination of Saccharomyces cerevisiae cell wall composition and beta-1,6-glucan fine structure. *Anal Biochem* 301(1):136–50.
6. Ciucanu I, Kerek F (1984) A simple and rapid method for the permethylation of carbohydrates. *Carbohydr Res* 131(2):209–217.
7. Ciucanu I (2006) Per-O-methylation reaction for structural analysis of carbohydrates by mass spectrometry. *Anal Chim Acta* 576(2):147–155.
8. Voiniciuc C, Günl M (2016) Analysis of Monosaccharides in Total Mucilage Extractable from Arabidopsis Seeds. *Bio-protocol* 6(9):e1801.
9. Foster CE, Martin TM, Pauly M (2010) Comprehensive Compositional Analysis of Plant Cell Walls (Lignocellulosic biomass) Part II: Carbohydrates. *J Vis Exp* 37(37):e1745.
10. Voiniciuc C (2017) Whole-seed Immunolabeling of Arabidopsis Mucilage Polysaccharides. *Bio-protocol* 7(11):e2323.
11. Voiniciuc C, Günl M, Schmidt MH-W, Usadel B (2015) Highly Branched Xylan Made by IRREGULAR XYLEM14 and MUCILAGE-RELATED21 Links Mucilage to Arabidopsis Seeds. *Plant Physiol* 169(4):2481–95.
12. Marcus SE, et al. (2010) Restricted access of proteins to mannan polysaccharides in intact plant cell walls. *Plant J* 64(2):191–203.
13. Tong Z (2011) Yeast Vacuole Staining with FM4-64. *BIO-PROTOCOL* 1(1). doi:10.21769/BioProtoc.18.
14. Schindelin J, et al. (2012) Fiji: an open-source platform for biological-image analysis. *Nat Methods* 9(7):676–682.
15. Abad S, et al. (2010) Real-time PCR-based determination of gene copy numbers in Pichia pastoris. *Biotechnol J*. doi:10.1002/biot.200900233.
16. Rebnegger C, et al. (2014) In Pichia pastoris, growth rate regulates protein synthesis and secretion, mating and stress response. *Biotechnol J* 9(4):511–525.
17. Pfaffl MW (2001) A new mathematical model for relative quantification in real-time RT-PCR. *Nucleic Acids Res* 29(9):e45.
18. Fraga D, Meulia T, Fenster S (2008) Real-Time PCR. *Current Protocols Essential Laboratory Techniques*, eds Gallagher SR, Wiley EA (John Wiley & Sons, Inc., Hoboken), pp 1–33. First Edit.
19. Ye J, et al. (2012) Primer-BLAST: A tool to design target-specific primers for polymerase chain reaction. *BMC Bioinformatics* 13(1):134.
20. Arvidsson S, Kwasniewski M, Riaño-Pachón DM, Mueller-Roeber B (2008) QuantPrime--a flexible tool for reliable high-throughput primer design for quantitative PCR. *BMC Bioinformatics* 9:465.